

Molecular analysis of aortic intimal hyperplasia caused by *Porphyromonas gingivalis* infection in mice with endothelial damage

K. Hokamura^{1*}, H. Inaba^{2*},
K. Nakano^{3*}, R. Nomura³,
H. Yoshioka⁴, K. Taniguchi⁵,
T. Ooshima³, K. Wada⁶, A. Amano²,
K. Umemura¹

¹Department of Pharmacology, Hamamatsu University School of Medicine, Hamamatsu, Japan, Departments of ²Oral Frontier Biology, ³Pediatric Dentistry, Osaka University Graduate School of Dentistry, Suita, Japan, Departments of ⁴Dentistry and Oral Surgery, ⁵Cardiovascular Surgery, Osaka Rosai Hospital, Sakai, Japan and ⁶Departments of Pharmacology, Osaka University Graduate School of Dentistry, Suita, Japan

Hokamura K, Inaba H, Nakano K, Nomura R, Yoshioka H, Taniguchi K, Ooshima T, Wada K, Amano A, Umemura K. Molecular analysis of aortic intimal hyperplasia caused by *Porphyromonas gingivalis* infection in mice with endothelial damage. *J Periodont Res* 2010; 45: 337–344. © 2009 John Wiley & Sons A/S

Background and Objective: *Porphyromonas gingivalis* infection is thought to be a significant etiological factor in the development of cardiovascular diseases. However, scant definitive evidence has been presented concerning the pathological molecular mechanisms of these disorders. In the present study, we performed a molecular analysis of the developmental mechanisms of aortic intimal hyperplasia induced by *P. gingivalis*.

Material and Methods: The effects of *P. gingivalis*-induced bacteremia on intimal hyperplasia were evaluated using a mouse model of aortic hyperplasia created by photochemical-induced endothelial cell injury. Alterations of gene expression profiles in injured blood vessels of the mice were extensively analyzed using DNA microarray assays to identify the key molecules involved in *P. gingivalis*-induced hyperplasia. In addition, human aneurismal specimens from patients with or without *P. gingivalis* infection were analyzed histochemically.

Results: Intravenous administration of *P. gingivalis* dramatically induced intimal hyperplasia in the mouse model. Concomitantly, S100 calcium-binding protein A9 (S100A9) and embryonic isoform of myosin heavy chain (SMemb), a proliferative phenotypic marker of smooth muscle cells, were significantly over-expressed on the surfaces of smooth muscle cells present in the injured blood vessels. Similarly, increased expressions of S100A9 and SMemb proteins were observed in aneurismal specimens obtained from *P. gingivalis*-infected patients.

Conclusion: We found that bacteremia induced by *P. gingivalis* leads to intimal hyperplasia associated with overexpressions of S100A9 and SMemb. Our results strongly suggest that oral–hematogenous spreading of *P. gingivalis* is a causative event in the development of aortic hyperplasia in periodontitis patients.

Dr Kazuhiko Nakano, DDS, PhD,
Department of Pediatric Dentistry, Osaka
University Graduate School of Dentistry, 1-8
Yamada-oka, Suita, Osaka 565-0871, Japan
Tel: +81 6 6879 2963
Fax: +81 6 6879 2965
e-mail: nakano@dent.osaka-u.ac.jp
*These authors contributed equally.

Key words: *Porphyromonas gingivalis*;
hyperplasia; aorta; mouse

Accepted for publication June 2, 2009

An epidemiological association between periodontal and cardiovascular diseases has emerged in recent studies (1). *Porphyromonas gingivalis* is con-

sidered to be one of the most important pathogens involved in several types of periodontal diseases (2). In addition, the bacterium is gaining increasing

attention for its possible association with cardiovascular diseases, and several epidemiological studies have strongly indicated its involvement in

the development of atherosclerosis and aneurysms (3,4). The mechanistic basis for causal association between *P. gingivalis* and cardiovascular disease has yet to be defined; however, within the confines of periodontal tissues, various bacteria and their antigens may initiate inflammatory responses with systemic consequences that could trigger cardiovascular diseases (5,6). Alternatively, direct oral-hematogenous spreading of bacteria to cardiovascular tissues may also occur. Bacteremia is a common condition often associated with tooth brushing and dental treatment (7–9). Furthermore, *P. gingivalis*, which is resistant to complement-mediated killing, is known to be able to survive within the bloodstream (10,11), while recent *in vitro* and *in vivo* studies have suggested that the bacterium possesses several properties possibly related to the pathogenesis of atherosclerosis (12,13). *P. gingivalis* has also been detected within human atherosclerotic specimens obtained from various ethnic groups (14–16), indicating the possibility that certain etiologies are involved in the development of aortic aneurysms and atherosclerosis mediated by *P. gingivalis*. However, it remains unclear how *P. gingivalis* is involved in the development of atherosclerosis and aneurysms.

In our recent study, cultured human aortic smooth muscle cells exposed to supernatants of blood plasma incubated with *P. gingivalis* showed a marked transformation from the contractile to the proliferative phenotype (17). The vascular endothelial layers are consistently injured directly and indirectly by various products, such as oxidized low-density lipids, inflammatory cytokines, glycation end-products, homocysteine and reactive oxygen species (18–20). The endothelial damage is one of the critical factors that trigger the onset of cardiovascular diseases, and may allow direct interaction of vascular smooth muscle cells with *P. gingivalis* in the blood. In the present study, we performed a molecular analysis of the developmental mechanisms of aortic hyperplasia induced by *P. gingivalis*, using an *in vivo* mouse model created by photochemical-induced endothelial damage.

We evaluated the virulence ability of *P. gingivalis* as well as *Streptococcus mutans*, a major pathogen of dental caries, to develop atherosclerosis in the mouse model, since *S. mutans* was previously detected at a high frequency in human atherosclerotic specimens (16). Next, alterations of gene expression profiles in injured blood vessels of mice were extensively evaluated using DNA microarray assays to identify the key molecules involved in this *P. gingivalis*-induced disorder. Finally, aneurismal clinical specimens were obtained from patients with or without *P. gingivalis* infection and histochemically analyzed to examine the involvement of the host molecules revealed in the DNA microarray assay results.

Material and methods

Bacterial strains

Porphyromonas gingivalis OMZ314, which was demonstrated to be a highly virulent strain in a mouse abscess model in our previous study (21), was grown anaerobically at 37°C in Tryptic

Soy Broth (Becton Dickinson, Sparks, MD, USA) supplemented with yeast extract (1 mg/mL), menadione (1 µg/mL) and hemin (5 µg/mL), as described previously (22). *S. mutans* TW871, isolated from the blood of a patient with infective endocarditis complicated with subarachnoid hemorrhage, was cultured in static conditions aerobically at 37°C in Brain Heart Infusion Broth (Becton Dickinson), as described previously (23,24). The tested strains were washed and adjusted to 1×10^9 colony-forming units/mL with phosphate-buffered saline.

Evaluation of intimal hyperplasia in mouse model

The present animal experiments conformed to the *Guide for the Care and Use of Laboratory Animals* published by the US National Institutes of Health (NIH publication no. 85-23, revised 1996), and were approved by the institutional animal care and use committees of Osaka University Graduate School of Dentistry and

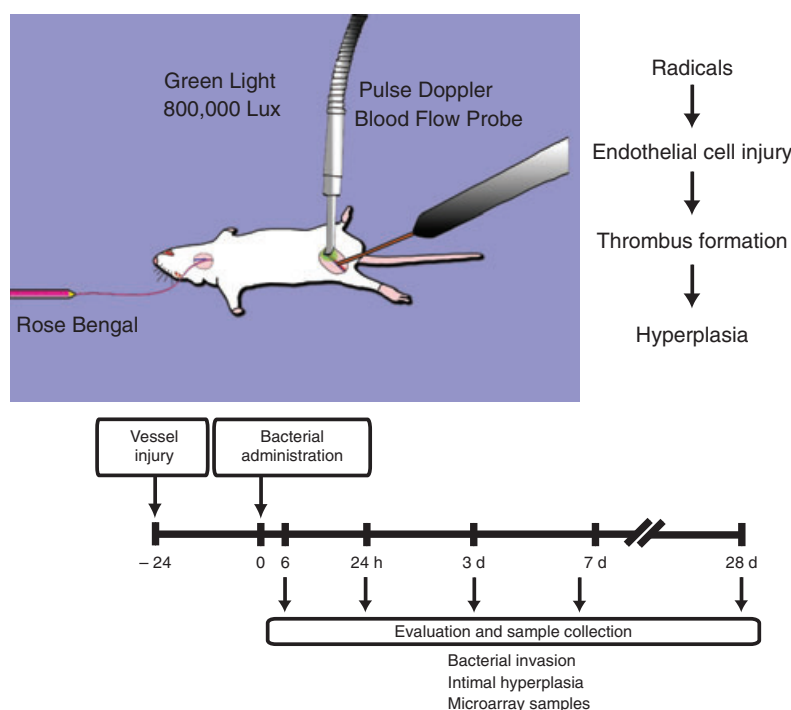


Fig. 1. Schematic illustration and protocol of photochemical-induced mouse femoral artery hyperplasia model. Photochemical-induced endothelial cell injury causes temporary thrombus formation, which is solved by endogenous fibrinolysis, after which smooth muscle cell-dependent intimal hyperplasia develops within 4–6 weeks.

Hamamatsu University School of Medicine. Endothelial injury in femoral arteries of mice was induced using a photochemical method, described previously, with some modifications (Fig. 1; 25,26). Briefly, male ICR mice (body weight, approximately 25–30 g; Japan SLC, Inc., Hamamatsu, Japan) were re-anesthetized with sodium pentobarbital, and then the right jugular vein was cannulated with a polyethylene tube for administration of Rose Bengal (photosensitizer). The right femoral artery was carefully exposed, and the probe of a pulse Doppler blood velocimeter was attached to the surface of the artery for monitoring blood flow. Photo-irradiation was executed with a xenon lamp equipped with a heat-absorbing filter (wavelength 540 nm; Hamamatsu Photonics, Hamamatsu, Japan) for 20 min, with Rose Bengal infusion (10 mg/kg) during the first 5 min. Formation of an occlusive thrombus resulting from the vessel injury was indicated by complete cessation of blood flow in the blood vessel. After the surgical operation, mice were immediately recovered, and were placed in the cage. Twenty-four hours after vessel injury, mice were anesthetized with sodium pentobarbital, bacterial suspensions (10^7 cells per mouse) in phosphate-buffered saline were intravenously administered via the jugular vein.

Intimal hyperplasia was evaluated 28 d after injection of the bacteria according to the method described in our previous reports, with some modifications (25,26). In brief, the blood vessels were extirpated after the mice were sacrificed by over dose anesthesia, and all arterial segments were sectioned transversely (4- μ m-thick sections at 0.3 mm intervals) and stained with Masson's trichrome. The intimal and medial areas were measured with the aid of a computer analysis system (DP controller, model DP70, Olympus, Tokyo, Japan), and the intima/media ratio was calculated as the average of three consecutive slices showing maximal intimal hyperplasia in the center of each area of damage among the serial sections.

Detection of *P. gingivalis* in the blood vessels was carried out as follows. Whole DNA was extracted from injured

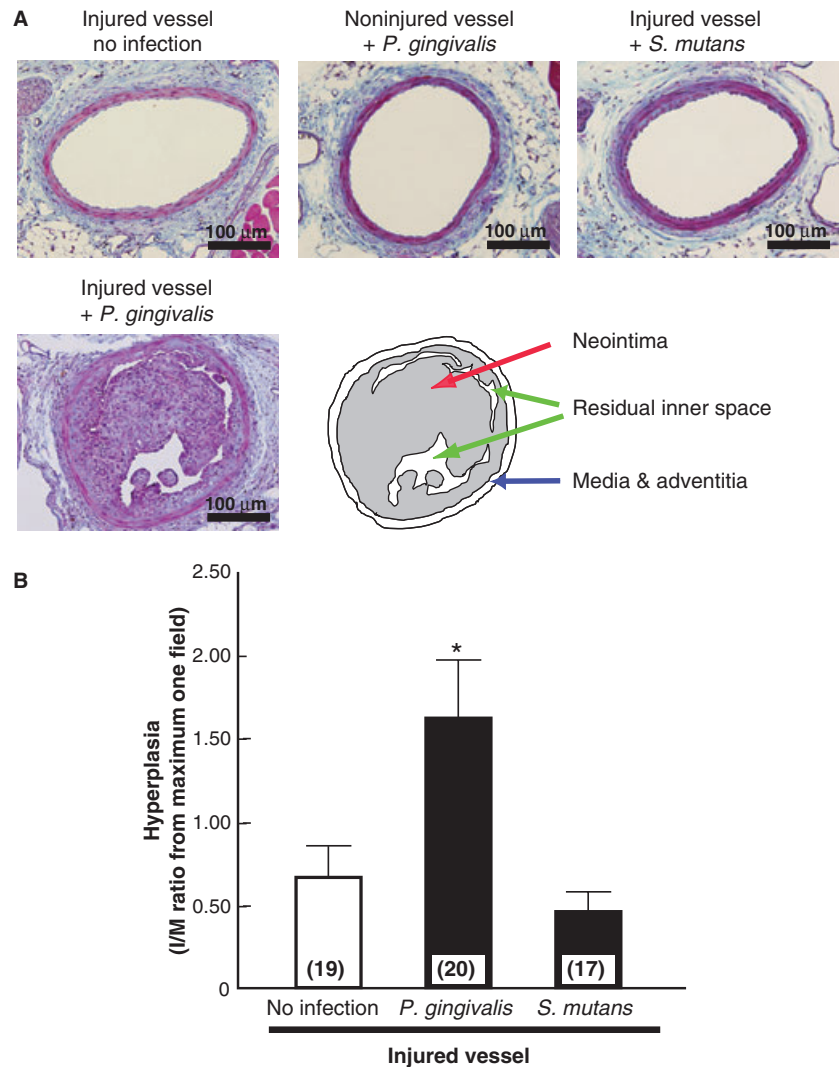


Fig. 2. Intimal hyperplasia of the aorta induced by oral bacterial infection after blood vessel injury. (A) Representative photomicrographs of intimal hyperplasia of the aorta induced by oral bacteria after blood vessel injury. Samples were collected from the mice 28 d after administration of the oral bacteria or vehicle. Tissue sections were stained with Masson's trichrome. The diagram provides a detailed description of hyperplasia induced by *P. gingivalis* administration. (B) Quantification of intimal hyperplasia in injured blood vessels 28 d after administration of *P. gingivalis*, *S. mutans* or the vehicle. The degree of intimal hyperplasia was calculated as the intima/media ratio (I/M ratio) from the maximum field prepared from each individual sample. Each column value represents the mean + SEM, and numbers in parentheses indicate the number of cases. * $p < 0.05$ vs. no infection.

and non-injured blood vessels extirpated at 6 h, 1, 3 or 7 d after bacterial injection, and polymerase chain reaction (PCR) was carried out according to a method described previously, with the limit of detection for bacteria from 5 to 50 cells in each specimen (16,27).

DNA microarray assays

Exhaustive analysis of gene alterations in injured blood vessels of the mice

was performed using a DNA microarray to investigate the molecules involved in *P. gingivalis*-induced vascular disease, according to a method described previously (28,29). Briefly, blood vessels were collected at 6 and 24 h after bacterial administration from three different groups of intimal hyperplasia model mice, then immediately snap-frozen in liquid nitrogen. In order to collect an adequate amount of RNA for microarray analysis, total

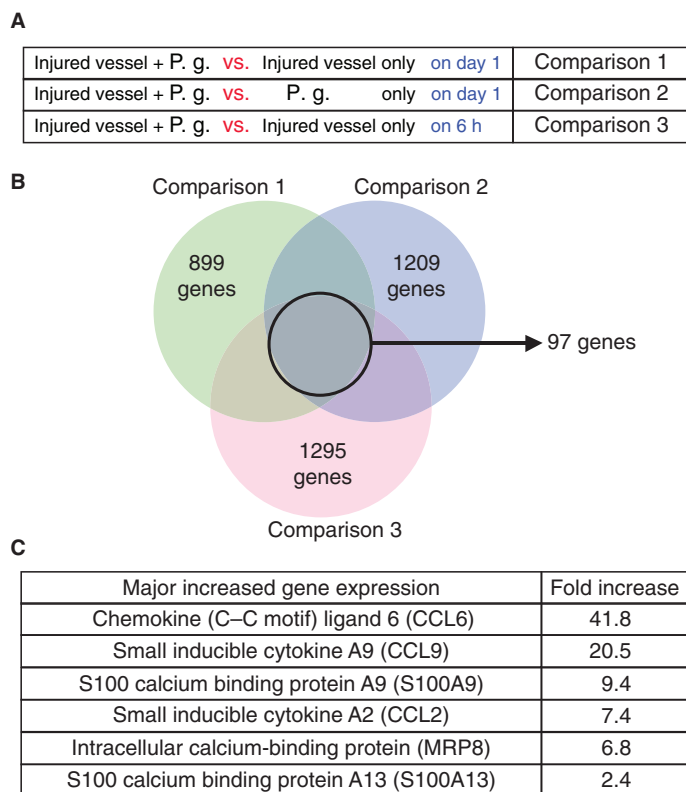


Fig. 3. Key molecules involved in intimal hyperplasia induced by *P. gingivalis* infection after blood vessel injury. (A) Comparison of three groups using DNA microarray assays. (B) The three groups shared 97 gene alterations in common. Since the range of glyceraldehyde-3-phosphate dehydrogenase (GAPDH, positive control) was from 0.8- to 1.2-fold, we evaluated changes greater than 1.5-fold or less than 0.5-fold as significant alterations. Altered genes in three different groups were compared, and 97 were nominated as the key molecules. (C) Among the 97 genes, those encoding chemokines and calcium-binding proteins, including S100A9, were found to account for the largest portion with an alteration > 2-fold.

RNA was prepared from tissues obtained from three mice in each group and mixed. Amino-allyl amplified RNA was then obtained from total RNA using an Amino-allyl MessageAmp aRNA kit (Ambion, Inc., Austin, TX, USA). Amino-allyl amplified RNA samples from each group were labelled with Cy3 or Cy5 using FluoroLink Cy3 or Cy5 mono-functional Dye 5-Packs (Amersham Bioscience, London, UK), then applied to a mouse gene chip system (Sigma Genosis Japan, Sapporo, Japan). The expression of genes was detected by the fluorescence intensity of Cy3 and Cy5. After normalization, gene alterations were determined from the ratio of Cy3 and Cy5, and expressed as fold increase in injured vessels with *P. gingivalis*, and compared with injured vessels without

infection and non-injured vessels with *P. gingivalis* infection. The range of glyceraldehyde-3-phosphate dehydrogenase (GAPDH, positive control) was from 0.8- to 1.2-fold; therefore, we evaluated changes greater than 1.5-fold or less than 0.5-fold as significant alterations. Altered genes were determined using three different comparisons: injured vessels with *P. gingivalis* infection vs. injured vessels without infection after 1 d; injured vessels with *P. gingivalis* infection vs. non-injured vessels with *P. gingivalis* infection after 1 d; and injured vessels with *P. gingivalis* infection vs. injured vessels without infection after 6 h.

Immunohistochemistry

The tissue sections were subjected to a standard immunohistochemical tech-

nique to detect the expression of chemokine ligand (CCL) 6, CCL9, S100A9 and SMemb, a proliferative phenotype marker of smooth muscle cells (30), using antibodies specific for each. Anti-CCL6 and -CCL9 antibodies were purchased from R&D Systems (Minneapolis, MN, USA), while anti-S100A9 polyclonal antibody was purchased from Santa Cruz Biotechnology, Inc. (Santa Cruz, CA, USA) and anti-non-muscle myosin heavy chain (SMemb) antibody from Yamasa Co. Ltd, (Choshi, Chiba, Japan). A Vectastain ABC kit (Vector Laboratories, Burlingame, CA, USA) was used with a diaminobenzidine substrate kit according to the manufacturer's instructions. Immunohistochemical detection of proliferating cell nuclear antigen (PCNA) to demonstrate active cellular proliferation was performed using a PCNA detection kit (Zymed Laboratories, South San Francisco, CA, USA).

Human tissue specimens for immunohistochemical staining of S100A9

Tissue sections processed from blood vessels of patients with aneurysms were obtained from surgical resection procedures performed at Osaka Rosai Hospital. This investigation conformed with the principles outlined in the Declaration of Helsinki, the study protocol was approved by the Ethics Committee of Osaka Rosai Hospital and written informed consent was obtained from the patients prior to collecting the specimens. Bacterial DNA in dental plaque and atheromatous specimens was extracted, followed by PCR detection of *P. gingivalis* bacterial DNA, as described previously (16). Subjects with *P. gingivalis* detected in either dental plaque or atheromatous specimens were classified as *P. gingivalis* positive, while those without detection of *P. gingivalis* in those specimens were classified as *P. gingivalis* negative. Several typical aneurismal lesions in each case were selected, and immunohistochemical staining for S100A9 was performed using anti-S100A9 polyclonal antibody.

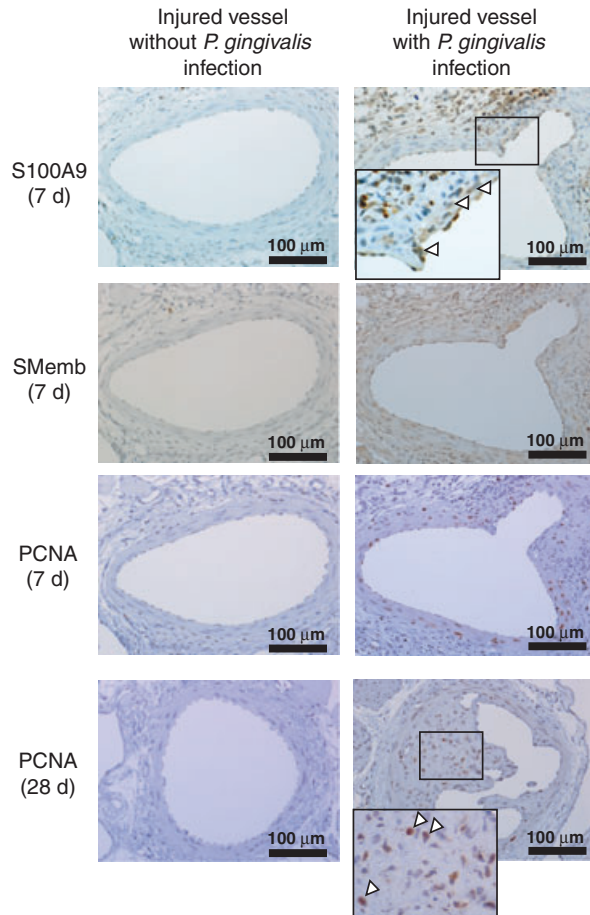


Fig. 4. Immunohistochemical staining of S100A9, SMemb and proliferating cell-nuclear antigen (PCNA) in areas of intimal hyperplasia induced by *P. gingivalis* infection after blood vessel injury. Immunohistochemical staining was performed for the detection of S100A9, SMemb and PCNA in the injured vessels of the mice at 7 and 28 d after administration of *P. gingivalis* or the vehicle. The target molecules are shown in brown. White arrowheads in the inset in the top panel represent smooth muscle cells stained with S100A9. White arrowheads in the bottom panel represent proliferating smooth muscle cells after 28 d stained with PCNA.

Statistical analysis

All results are expressed as the means \pm SEM. Statistical comparisons were made using Student's unpaired *t*-test or Scheffe's method after analysis of variances (ANOVA). The results were considered significantly different at $p < 0.05$.

Results

Formation of aortic intimal hyperplasia in mouse model

Bacteremia caused by *P. gingivalis* induced considerable formations of aortic intimal hyperplasia in the

injured vessels after 28 d, as shown in Fig. 2. Neointimal lesions were most common in the areas affected by hyperplasia (Fig. 2A). In contrast, hyperplasia was rarely observed in injured vessels without *P. gingivalis* infection or in non-injured vessels with infection (Fig. 2B). In addition, only slight hyperplasia was induced in vessels injured following *S. mutans* infection (Fig. 2B). The PCR analyses demonstrated that both *P. gingivalis* and *S. mutans* were present in the photochemically injured blood vessels extirpated at 6 h, 1, 3 and 7 d after bacterial injection, whereas the infected bacteria were rarely detected in the non-injured blood vessels (data not

shown). These results suggest that bacteremia induced by *P. gingivalis* can lead to aortic intimal hyperplasia, and endothelial injury is essential for lesion formation. In contrast, the etiology of disease caused by *S. mutans* was not demonstrated in this model.

Key molecules involved in intimal hyperplasia induced by *P. gingivalis* in blood

Alterations of gene expression profiles in injured blood vessels of the mice were extensively performed using DNA microarray analysis to identify the key molecules involved in *P. gingivalis*-induced hyperplasia. To reduce the confounding effects of false signals, we compared the results obtained in three different conditions (Fig. 3A) and found significant alterations of 97 genes (Fig. 3B). Among the 97 genes, those encoding chemokines and calcium-binding proteins, including S100A9, were found to account for the largest portion, as shown in Fig. 3C.

Next, altered expressions of these potential molecules were examined using immunohistochemical staining of blood vessel specimens from the mice. Overexpressions of CCL6 and CCL9 were observed in the injured blood vessels at 6 h after *P. gingivalis* infection, whereas such overexpressions were negligibly observed in the non-injured vessels with and without *P. gingivalis* infection (data not shown). However, the overexpressions of CCL6 and CCL9 disappeared at 7 d after bacterial infection (data not shown). In contrast, enhanced expression of S100A9 was continuously observed from the early phase (6 h) to 7 d after infection with *P. gingivalis* (Fig. 4). In addition, S100A9 expression was frequently localized in proliferating smooth muscle cells at 7 d after infection. Furthermore, the expression of SMemb was observed in smooth muscle cells in the injured vessels at 7 d after the bacterial infection. The expression of proliferating cell nuclear antigen (PCNA), a marker of cell proliferation, was also examined to confirm cellular proliferation, and strong expression was found in injured

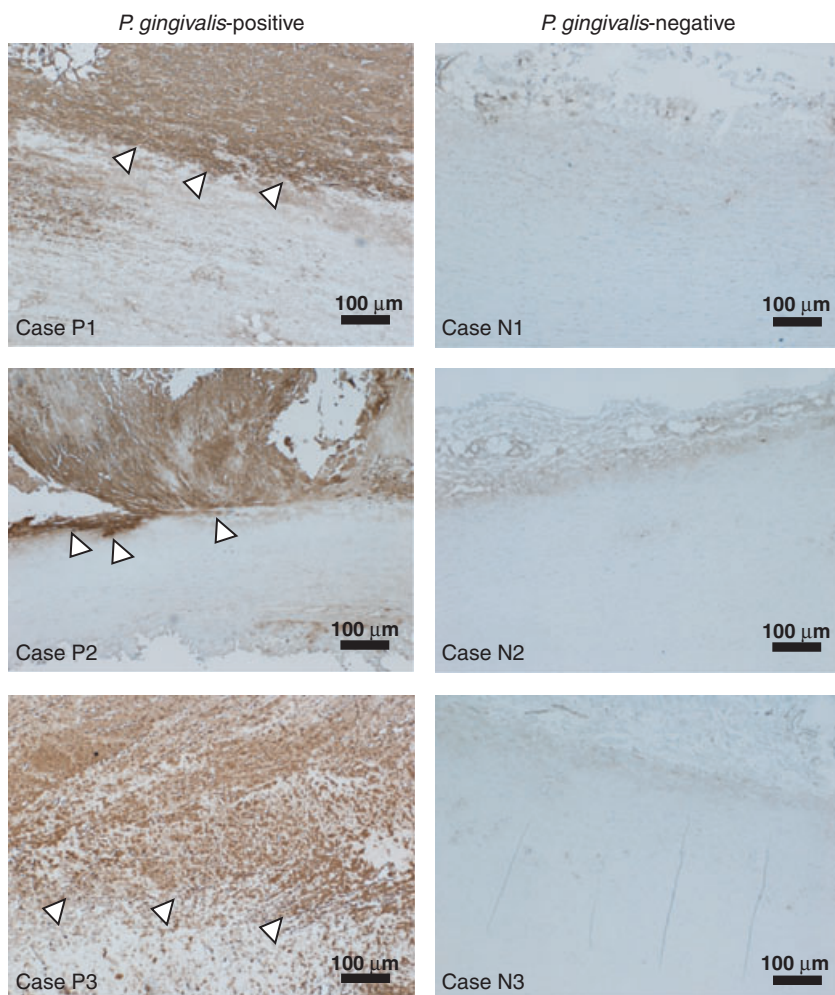


Fig. 5. Immunohistochemical detection of S100A9 expression in aortic aneurismal lesions from patients with or without *P. gingivalis* infection. Representative photographs of aneurismal lesions from *P. gingivalis*-positive (cases P1–P3) and *P. gingivalis*-negative patients (cases N1–N3) are shown. Brown coloration (indicated by arrowheads) shows S100A9 expression.

vessels with *P. gingivalis* infection from 7 to 28 d after bacteria infection, but not in injured vessels without infection (Fig. 4). The expressions of S100A9, SMemb and PCNA seemed to be co-localized in the vascular tissues.

Overexpression of S100A9 protein in cardiovascular lesions of patients infected with *P. gingivalis*

We analyzed 12 *P. gingivalis*-positive specimens and 12 *P. gingivalis*-negative specimens, among which six representative specimens are shown in Fig. 5. In all 12 of the *P. gingivalis*-positive specimens S100A9 was identified, and strong expression was observed in 10.

In contrast, there were few *P. gingivalis*-negative specimens with a positive expression of S100A9. Expression of S100A9 was localized in areas corresponding to proliferating smooth muscle cells and co-localized with SMemb (data not shown).

Discussion

In the present study, we evaluated the etiology of atherosclerosis development caused by *P. gingivalis* as well as *S. mutans* in a mouse model with photochemical-induced endothelial damage. *P. gingivalis* in the blood caused formation of considerable intimal hyperplasia in photochemical-

damaged blood vessels, whereas *S. mutans* did not. Furthermore, aortic intimal hyperplasia was formed in regions with proliferative smooth muscle cells and was associated with overexpression of S100A9 and SMemb. It should be noted that these mice did not suffer from any type of hypercholesterolemia. Therefore, the present findings suggest direct involvement of *P. gingivalis* in the development of vascular disease without hypercholesterolemia, which is a novel pathological molecular mechanism of cardiovascular diseases.

A previous study found that oral infection with *P. gingivalis* accelerated early atherosclerosis in hypercholesterolemic apolipoprotein-E null mice, whereas the disorder was not seen in wild-type mice with *P. gingivalis* infection (31), suggesting that hypercholesterolemia is essential for atherosclerosis associated with *P. gingivalis* infection. Our results, however, showed that *P. gingivalis* induces intimal hyperplasia without host hypercholesterolemia. Although the distinct molecular mechanisms involved in this discrepancy should be analyzed further in detail, other reports have noted that Burger's disease, an occlusive vascular disease, occurs in individuals infected with *P. gingivalis*, despite the absence of cholesterol elevation in plasma (32–34), which supports the present findings. Another intriguing finding is that *P. gingivalis* in the bloodstream fails to gain access to the vessel wall across the uninjured endothelial layer. As mentioned in the Introduction, the endothelial layers are frequently injured in conditions caused by various substances in blood. It is also known that smoking induces free radical generation in blood, which injures endothelial layers and is considered the most important risk factor for Burger's disease (33,35). Thus, *P. gingivalis* in the bloodstream is likely to invade damaged endothelial layers, allowing direct interaction with vascular smooth muscle cells, which may trigger the onset of cardiovascular diseases.

According to the present DNA microarray results, we focused on chemokines and S100 calcium-binding proteins. The CC chemokine ligands

CCL6 and CCL9 have been reported to elicit various inflammatory responses (36). However, the increased expressions of those chemokine ligands in injured blood vessels of mice induced by *P. gingivalis* were diminished within 7 d. Therefore, it is suggested that CC chemokine ligands play a role as initiators or accelerators of vascular injury in the early phase, but may not be key molecules in the development of intimal hyperplasia. In contrast, the increased expression of S100 calcium-binding proteins, especially S100A9, persisted until 28 d after the bacterial infection. These results led us to speculate that upregulation of S100A9 by smooth muscle cells is an important factor involved in the induction of intimal hyperplasia in the aorta by *P. gingivalis*.

Although it has been reported that S100A9 is a member of the S100 calcium-binding protein family, its biological roles and functional mechanisms remain unclear (37). Since the expression of S100A9 has been observed in inflammation and cancer lesions, it has been suggested that the protein plays an important role in cellular proliferation (38). In addition, we recently reported that S100A9 expression was observed following *P. gingivalis* infection of primary human aortic smooth muscle cells with cellular proliferation, and knockdown of S100A9 by small interfering RNA dramatically attenuated both the phenotypic changes and proliferation (17). In the present *in vivo* experimental conditions, overexpression of S100A9 was observed in smooth muscle cells in the intimal and medial layers. Therefore, it is suggested that ectopic expression of S100A9 in smooth muscle cells causes phenotypic transformation from contractile to proliferative as well as hyperplastic growth of smooth muscle cells migrating to the intimal area.

We also detected a strong expression of S100A9 protein in tissue sections processed from aneurysmal blood vessels of *P. gingivalis*-positive patients but not in those from *P. gingivalis*-negative patients. These observations support the present results and suggest that upregulation of S100A9 by

P. gingivalis is involved in the development of cardiovascular lesions induced by the bacterium, such as aneurysms, aortic hyperplasia and atherosclerosis.

In conclusion, we found that infection of endothelial-damaged vessels by *P. gingivalis* dramatically induced proliferation of smooth muscle cells, leading to intimal hyperplasia without hypercholesterolemia. Our results suggest that upregulation of S100A9 and SMemb by *P. gingivalis* is an important event in the development of aortic intimal hyperplasia.

Acknowledgements

This study was supported in part by grants (19209063 to T.O., 18592028 to K.W., 18791347 to H.I. and 18689050 to K.N.) from the Japan Society for the Promotion of Science, as well as a grant from the Center of Excellence program entitled 'Origination of Frontier Bi-Dentistry' held at Osaka University Graduate School of Dentistry. We thank Dr K. Katayama, Department of Pharmacology, Osaka University Graduate School of Dentistry, for technical support. We also appreciate Professor Y. Kamisaki, Department of Pharmacology, Osaka University Graduate School of Dentistry, and Professor A. Nakajima, Gastroenterology Division, Yokohama City University School of Medicine, for their supervision of the study.

References

1. Meurman JH, Sanz M, Janket SJ. Oral health, atherosclerosis, and cardiovascular disease. *Crit Rev Oral Biol Med* 2004; **15**:403–413.
2. Pihlstrom BL, Michalowicz BS, Johnson NW. Periodontal diseases. *Lancet* 2005; **366**:1809–1820.
3. Scannapieco FA, Bush RB, Paju S. Associations between periodontal disease and risk for atherosclerosis, cardiovascular disease, and stroke. A systematic review. *Ann Periodontol* 2003; **8**:38–53.
4. D'Aiuto F, Parkar M, Andreaou G, Brett PM, Ready D, Tonetti MS. Periodontitis and atherogenesis: causal association or simple coincidence? *J Clin Periodontol* 2004; **31**:402–411.
5. Beck J, Garcia R, Heiss G, Vokonas PS, Offenbacher S. Periodontal disease and

- cardiovascular disease. *J Periodontol* 1996; **67**:1123–1137.
6. Garcia RI, Henshaw MM, Krall EA. Relationship between periodontal disease and systemic health. *Periodontol* 2000 2001; **25**:21–36.
7. Kinane DF, Riggo MP, Walker KF, MacKenzie D, Shearer B. Bacteraemia following periodontal procedures. *J Clin Periodontol* 2005; **32**:708–713.
8. Lockhart PB, Brennan MT, Sasser HC, Fox PC, Paster BJ, Bahrani-Mougeot FK. Bacteremia associated with toothbrushing and dental extraction. *Circulation* 2008; **117**:3118–3125.
9. Pérez-Chaparro PJ, Gracieux P, Lafaurie GI, Donnio PY, Bonnaure-Mallet M. Genotypic characterization of *Porphyromonas gingivalis* isolated from subgingival plaque and blood sample in positive bacteremia subjects with periodontitis. *J Clin Periodontol* 2008; **35**:748–753.
10. Slaney JM, Gallagher A, Aduse-Opoku J, Pell K, Curtis MA. Mechanisms of resistance of *Porphyromonas gingivalis* to killing by serum complement. *Infect Immun* 2006; **74**:5352–5361.
11. Potempa M, Potempa J, Okroj M *et al*. Binding of complement inhibitor C4b-binding protein contributes to serum resistance of *Porphyromonas gingivalis*. *J Immunol* 2008; **181**:5537–5544.
12. Kuramitsu HK, Qi M, Kang IC, Chen W. Role for periodontal bacteria in cardiovascular diseases. *Ann Periodontol* 2001; **6**:41–47.
13. Li L, Messas E, Batista EL Jr, Levine RA, Amar S. *Porphyromonas gingivalis* infection accelerates the progression of atherosclerosis in a heterozygous apolipoprotein E-deficient murine model. *Circulation* 2002; **105**:861–867.
14. Haraszthy VI, Zambon JJ, Trevisan M, Zeid M, Genco RJ. Identification of periodontal pathogens in atheromatous plaques. *J Periodontol* 2000; **71**:1554–1560.
15. Kozarov E, Sweier D, Shelburne C, Progulsk-Fox A, Lopatin D. Detection of bacterial DNA in atheromatous plaques by quantitative PCR. *Microbes Infect* 2006; **8**:687–693.
16. Nakano K, Inaba H, Nomura R *et al*. Detection of cariogenic *Streptococcus mutans* in extirpated heart valve and atheromatous plaque specimens. *J Clin Microbiol* 2006; **44**:3313–3317.
17. Inaba H, Hokamura K, Nakano K *et al*. Upregulation of S100 calcium-binding protein A9 is required for induction of smooth muscle cell proliferation by a periodontal pathogen. *FEBS Lett* 2009; **583**:128–134.
18. Papatheodorou L, Weiss N. Vascular oxidant stress and inflammation in hyperhomocysteinemia. *Antioxid Redox Signal* 2007; **9**:1941–1958.

19. Esper RJ, Vilariño JO, Machado RA, Paragano A. Endothelial dysfunction in normal and abnormal glucose metabolism. *Adv Cardiol* 2008;**45**:17–43.
20. Fisher M. Injuries to the vascular endothelium: vascular wall and endothelial dysfunction. *Rev Neurol Dis* 2008;**5**: S4–S11.
21. Nakano K, Kuboniwa M, Nakagawa I et al. Comparison of inflammatory changes caused by *Porphyromonas gingivalis* with distinct *fimA* genotypes in a mouse abscess model. *Oral Microbiol Immunol* 2004;**19**:205–209.
22. Inaba H, Kawai S, Kato T, Nakagawa I, Amano A. Association between epithelial cell death and invasion by microspheres conjugated to *Porphyromonas gingivalis* vesicles with different types of fimbriae. *Infect Immun* 2006;**74**:734–739.
23. Nakano K, Nomura R, Nakagawa I, Hamada S, Ooshima T. Demonstration of *Streptococcus mutans* with a cell wall polysaccharide specific to a new serotype, *k*, in the human oral cavity. *J Clin Microbiol* 2004;**42**:198–202.
24. Nomura R, Nakano K, Nemoto H et al. Isolation and characterization of *Streptococcus mutans* in heart valve and dental plaque specimens from a patient with infective endocarditis. *J Med Microbiol* 2006;**55**:1135–1140.
25. Kikuchi S, Umemura K, Kondo K, San-iabadi AR, Nakashima M. Photochemically induced endothelial injury in the mouse as a screening model for inhibitors of vascular intimal thickening. *Arterioscler Thromb Vasc Biol* 1998;**18**:1069–1078.
26. Kondo K, Umemura K, Miyaji M, Nakashima M. Milrinone, a phosphodiesterase inhibitor, suppresses intimal thickening after photochemically induced endothelial injury in the mouse femoral artery. *Atherosclerosis* 1999;**142**:133–138.
27. Tran SD, Rudney JD. Multiplex PCR using conserved and species-specific 16S rRNA gene primers for simultaneous detection of *Actinobacillus actinomycetemcomitans* and *Porphyromonas gingivalis*. *J Clin Microbiol* 1996;**34**: 2674–2678.
28. Wada K, Arita M, Nakajima A et al. Leukotriene B4 and lipoxin A4 are regulatory signals for neural stem cell proliferation and differentiation. *FASEB J* 2006;**20**:1785–1792.
29. Tachibana M, Wada K, Katayama K et al. Activation of peroxisome proliferator-activated receptor gamma suppresses mast cell maturation involved in allergic diseases. *Allergy* 2008;**63**:1136–1147.
30. Nagai R, Kowase K, Kurabayashi M. Transcriptional regulation of smooth muscle phenotypic modulation. *Ann N Y Acad Sci* 2000;**902**:214–223.
31. Lalla E, Lamster LB, Hofmann MA et al. Oral infection with a periodontal pathogen accelerates early atherosclerosis in apolipoprotein E-null mice. *Arterioscler Thromb Vasc Biol* 2003;**23**:1405–1411.
32. Mishima Y. Thromboangiitis obliterans (Buerger's disease). *Int J Cardiol* 1996;**54**:S185–S187.
33. Roncon-Albuquerque R, Serrão P, Vale-Pereira R, Costa-Lima J, Roncon-Albuquerque R Jr. Plasma catecholamines in Buerger's disease: effects of cigarette smoking and surgical sympathectomy. *Eur J Vasc Endovasc Surg* 2002;**24**: 338–343.
34. Iwai T, Inoue Y, Umeda M et al. Oral bacteria in the occluded arteries of patients with Buerger disease. *J Vasc Surg* 2005;**42**:107–115.
35. Celermajer DS, Adams MR, Clarkson P et al. Passive smoking and impaired endothelium-dependent arterial dilatation in healthy young adults. *N Engl J Med* 1996;**334**:150–154.
36. IUIS/WHO Subcommittee on Chemokine Nomenclature. Chemokine/chemokine receptor nomenclature. *J Immunol Methods* 2002;**262**:1–3.
37. McCormick M, Rahimi MF, Bobryshev YV et al. S100A8 and S100A9 in human arterial wall. Implications for atherogenesis. *J Biol Chem* 2005;**280**: 41521–41529.
38. Gebhardt C, Németh J, Angel P, Hess J. S100A8 and S100A9 in inflammation and cancer. *Biochem Pharmacol* 2006;**72**: 1622–1631.

This document is a scanned copy of a printed document. No warranty is given about the accuracy of the copy. Users should refer to the original published version of the material.